Biosensors and Bioelectronics 26 (2010) 1098–1103

Contents lists available at ScienceDirect

Biosensors and Bioelectronics

journal homepage: www.elsevier.com/locate/bios

Amperometric glucose biosensor based on a triangular silver nanoprisms/chitosan composite film as immobilization matrix

Wentao Shi, Zhanfang Ma*

Department of Chemistry, Capital Normal University, No. 105 Xi San Huan North Rd., Beijing 100048, China

ARTICLE INFO

Article history:
Received 15 June 2010
Received in revised form 26 August 2010
Accepted 26 August 2010

Keywords:
Amperometric biosensor
Triangular silver nanoprism
Glucose oxidase
Dip-coating
Crosslinking

ABSTRACT

We report on the utilization of triangular silver nanoprisms (AgTNPs) to create a highly responsive glucose biosensor. Glucose oxidase (GOD) was simply mixed with AgTNPs and cross-linked on the Pt electrode with chitosan (CHIT) medium by glutaraldehyde. Circular dichroism (CD) and UV-spectrum results show that the activity of GOD was preserved after conjugating with AgTNPs. The current response of modified electrode is 16 times higher than that without AgTNPs. The biosensor showed high sensitivity (67.17 $\mu A\,cm^{-2}\,mM^{-1}$), low detection limit (1×10^{-6} M), good storage stability, and high affinity to glucose (K_M = 3.84 mM). A linear calibration plot was obtained in the wide concentration range from 3×10^{-6} to 3×10^{-3} M. The excellent performance of the biosensor is attributed to large surface-to-volume ratio and high conductivity of AgTNPs, and good biocompatibility of CHIT, which enhances the enzyme absorption and promotes electron transfer between redox enzymes and the surface of electrodes.

1. Introduction

Electrochemical biosensors based upon nanomaterials have recently attracted considerable attention (Pandey et al., 2008; Valentini and Palleschi, 2008; Willner et al., 2007). The electrochemical method has many advantages, such as high sensitivity, good selectivity, fast detection and low cost, therefore many electrochemical sensors with high sensitivity and selectivity toward many analytes have been prepared (Ahmed et al., 2008; Drummond et al., 2003). Among them, glucose biosensors would provide the possibility of carrying out analytical and diagnostic procedures simply and rapidly.

Nanoparticles have attracted much attention in the past few years due to their interesting physical and chemical properties and potential applications in many areas such as optics, electronics, magnetic devices, and catalyst (Thakar et al., 2007; Peng and Sun, 2007; Liang et al., 2004). Among them, sensor is one of the most useful sections. Recent studies have demonstrated that many nanomaterials, such as gold nanoparticles (Pingarron et al., 2008; Yanez-Sedeno and Pingarron, 2005), silver nanoparticles (AgNPs) (Ren et al., 2005; Wen et al., 2006; Gan et al., 2004), gold cluster (Xiao et al., 2003), quantum dots (Du et al., 2008), magnetic nanoparticles (Grancharov et al., 2005), carbon nanomaterials (Wen et al., 2007; Lee et al., 2005), hold great promise for the immobilization of biomolecules. Especially, AgNPs possess a strong ability for physical absorption which can absorb protein macromolecules like GOD (Ma et al., 2008); as a conductive metal, AgNPs can act as conductive wire between the interaction center and electrode (Wen et al., 2006); AgNPs have catalytic ability toward hydrogen peroxide (H_2O_2) which is produced by GOD oxidizing glucose (Gan et al., 2004; Campbell et al., 2009). These properties of AgNPs provide a suitable microenvironment for biomolecules immobilization retaining their biological activity, and facilitate electron transfer between the immobilized proteins and electrode substrates, which have led to an intensive use of AgNPs for the construction of electrochemical biosensors with enhanced analytical performance with respect to other biosensor designs (Ma et al., 2009a,b; Ren et al., 2005).

CHIT with abundant amino groups exhibits good biocompatibility (Liu et al., 2005) and excellent film-forming ability originating from its protonation and solubility in slightly acidic solution and stability from insolubility in solution with pH over pK_a (6.3) (Sorlier et al., 2001). Therefore, it is a very suitable matrix for immobilizing bioactive molecules and constructing biosensors.

It is now well-known that the anisotropic nanoparticles are particularly interesting because the decreased symmetry of such particles often leads to new and unusual chemical and physical behavior (Wang and Song, 2006). Within this class of particles, AgTNPs stand out due to their structure- and environment-dependent optical features, their anisotropic surface energetics (Pastoriza-Santos and LizMarzán, 2002). Jiang and Yu (2008) applied AgTNPs to detect halide ions, $H_2PO_4^-$ and SCN^- by the changing of the SPR when the ions were added to the AgTNPs solution and the detect ion limit can be up to 10^{-6} M. Wu et al. (2009) found that cysteine can

* Corresponding author.
E-mail address: mazhanfang@yahoo.com (Z. Ma).

0956-5663/$ – see front matter © 2010 Elsevier B.V. All rights reserved.
doi:10.1016/j.bios.2010.08.072

lead to blue shift of dipole plasmon resonance absorption of AgTNPs, but other 19 kinds of natural amino acids could not. Haes and Van Duyne (2002) pioneered using AgTNPs with 100 nm wide and 50 nm high prepared by Nanosphere Lithography method which was time-consuming and needed vacuum deposition system, and they successfully built a optical biosensor for detecting streptavidin by utilizing the localized surface plasmon resonance of AgTNPs. The AgTNPs prepared by sol–gel method were instable in strong acid, alkali or high ionic strength solution and this property seriously hindered its wide application. Xue et al. (2007) applied SiO_2 shell to protect AgTNPs for detecting DNA. So far, there is no report that AgTNPs prepared by sol–gel method were directly used for biosensing. Herein, the AgTNPs prepared by sol–gel were directly applied to enhance an amperometric glucose biosensor for the first time. After applying GOD to AgTNPs solution, measurements show that the surface interaction between them is close, and the activity of GOD is preserved after conjugating with AgTNPs. Amperometric measurement results show that the AgTNPs can significantly enhance the current sensitivity of GOD enzyme electrodes. The performance of the obtained electrodes with respect to linear range, reproducibility, response time, and stability is presented and discussed.

2. Experimental

2.1. Materials

GOD was extracted from *Aspergillus niger* (Fluka company, 211 U/mg), and used without further purification. Glucose and $AgNO_3$ are purchased from Alfa Aesar Co., Ltd, and sodium borohydride is purchased from Sigma Co., Ltd. Trisodium citrate, hydrogen peroxide, NaH_2PO_4, Na_2HPO_4, $K_4Fe(CN)_6$ and $K_3Fe(CN)_6$ are obtained from Beijing Chemical Reagents Company (Beijing, China). In all the procedures, the water used was purified through an Olst ultrapure K8 apparatus (Olst, Ltd., resistivity >18 MΩ).

2.2. Apparatus

Transmission electron microscopy (TEM) was performed with a JEOL-100CX electron microscope under 80 kV accelerating voltage. Absorption spectra were obtained by using a U-2550 spectrophotometer (Hitachi, Japan). The CD spectra were taken using a Jasco J-816 spectropolarimeter. Quartz cells of 1 mm optical path length were used for all CD spectra measurements of GOD (0.5 mg/mL) and GOD–AgTNPs solutions. The phosphate buffer (PB, Na_2HPO_4–NaH_2PO_4, pH 7.0) was used to prepare these solutions. The spectra were analyzed for the content of secondary structure by using the software accompanying the spectropolarimeter.

2.3. Preparation of AgTNPs

In a typical experiment, an aqueous solution of silver nitrate (0.1 mM, 25 mL), trisodium citrate (30 mM, 1.5 mL), and hydrogen peroxide (30 wt.%, 60 μL) were combined and vigorously stirred at room temperature in the presence of air. To this mixture, sodium borohydride (100 mM, 200 μL) was rapidly injected, generating a colloid that color turned blue eventually (as evidenced by UV–vis spectroscopy and the identification of the surface plasmon resonance). For a purpose of obtaining more evenly distributed AgTNPs, the stirring continued for another 30 min. The prepared AgTNPs was centrifuged to condense the solution for 10 times.

2.4. Preparation of enzyme electrodes

The platinum electrode (d = 1 mm, length = 10 mm) was polished with 0.05 μm alumina slurry, and then boiled in 6 mol L^{-1} HNO_3. Finally, the electrode was washed using double distilled water.

Dip-coating (Dave et al., 1998) and crosslinking (Krajewska, 2004) methods were employed to fabricate the enzyme electrode (CHIT/GOD@AgTNPs/Pt). A typical procedure was as follows: 0.06 mL of GOD solution (10 mg mL^{-1}) was mixed with 0.12 mL of condensed AgTNPs solution in a beaker. 5 min later, 0.8 mL of CHIT solution (1.0 wt.%, and the concentration of HAc was 83.3 mM) (Wang et al., 2002) and 0.02 mL of glutaraldehyde water solution (2.5 wt.%) were added to the beaker successively. The solution was mixed completely by a vortex for 5 min and then the platinum electrode was dipped into the mixture for 30 s. After that, the electrode was dried in air at room temperature to fabricate the enzyme electrode. The control enzyme electrode (CHIT/GOD/Pt) was made by immobilizing GOD to the platinum electrode without AgTNPs. The enzyme electrodes were stored at 4 °C prior to use. The amount of AgTNPs was estimated as follows: the concentration of prepared AgTNPs is 0.01 mg/mL, and after the centrifugation, the solution condenses to 0.1 mg/mL. After mixed with chitosan and other species, the concentration of AgTNPs becomes 0.012 mg/mL. The loading of AgTNPs is ca. 7×10^{-5} mg cm^{-2} by weighting the electrode before and after dip-coating.

2.5. Electrochemical measurements

The electrochemical measurements are performed on a CH Instruments 832 electrochemical analysis station (CHI-832, Chenhua, Shanghai, China) connected with a PC. Catalytic activity of immobilized GOD was tested by measuring the response current of the enzyme electrode. The experiment was carried out with a traditional three-electrode cell, a platinum wire as the counter electrode, a KCl-saturated Ag/AgCl (Ag/AgCl) as reference electrode and a modified enzyme electrode (fixed area, 0.1645 cm^2) as the working electrode. A fixed potential of 0.6 V was used to measure the response current. After the background current reached a steady-state value, different dose of glucose was injected into the phosphate buffer solution (0.1 mol L^{-1}, pH 7.0) and the response currents were recorded with time. All experiments were conducted at 35 °C.

3. Results and discussion

3.1. Characterization of biocomposite of GOD–AgTNPs

The edge lengths of AgTNPs used in this work are from ca. 20 nm to ca. 40 nm as shown in Fig. 1A. The UV absorption spectra of AgTNPs are given in Fig. 1B, there are three typical peaks 755, 542, and 332 nm, corresponding to in-plane dipole resonance, out-of-plane quadrupole resonance, and in-plane quadrupole resonance, respectively (Pastoriza-Santos and LizMarzán, 2002; Ma et al., 2009a,b) (curve *b*). The absorption spectra of pure GOD had absorption peak in the visible region with maximum values at 374 and 450 nm (curve *a*), which were consistent with previous report (Chi et al., 1994). For the triangular silver nanoprisms, after bioconjugation of GOD with AgTNPs (curve *c*), these absorption bands had slightly shifted to 777, 493 and 331 nm, respectively. The shifts of the absorbance maximum of GOD may attribute to the interaction between AgTNPs and GOD, which also indicates that GOD has been adsorbed on the surface of AgTNPs (Ren et al., 2009).

Recently, CD has been widely used to analyze the main properties and features of enzyme solutions and films (Shimizu et al., 2003). Therefore, CD spectra are used to characterize the secondary structure of GOD after bioconjugating with AgTNPs. Spectral analysis can be used to estimate the secondary structure content. The CD spectrum of GOD–Ag bioconjugates looks similar to that of the pure GOD, but the peak has slightly less intensity as

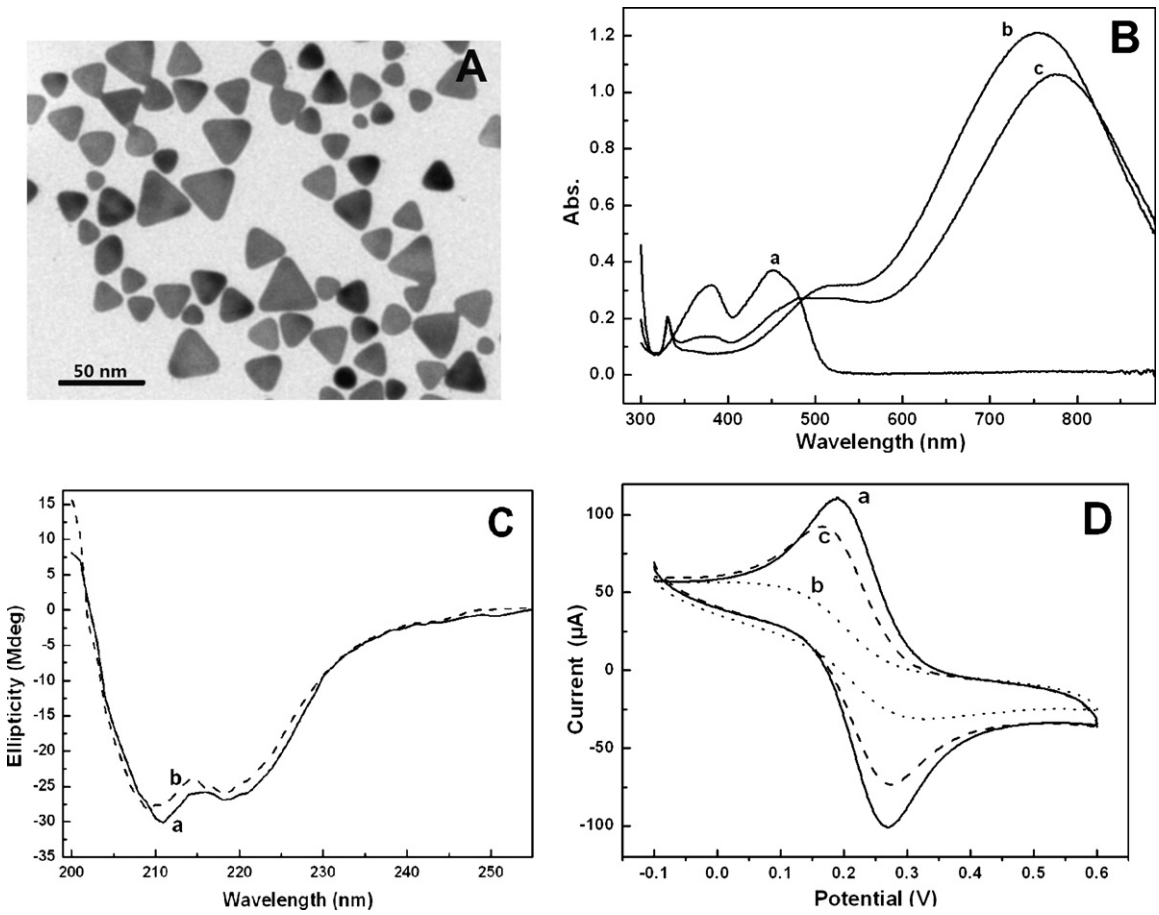

Fig. 1. (A) TEM image of AgTNPs; (B) UV–vis spectra of GOD (a), AgTNPs (b), and GOD–Ag bioconjugates (c); (C) CD spectra of pure GOD (a) and GOD–AgTNPs bioconjugates (b); (D) cyclic voltammograms (CVs) of different modified electrodes in 5.0 mM ferricyanide solution: (a) bare Pt electrode, (b) the electrode with CHIT film, (c) the electrode with CHIT film added GOD and AgTNPs (scan rate is 50 mV/s).

shown in Fig. 1C, indicating that the GOD have been adsorbed on the surface of AgTNPs and the secondary structure of GOD was preserved after conjugating with AgTNPs (Courrol et al., 2007). Meanwhile, to figure out the distribution of GOD and AgTNPs, atomic force microscopy (AFM) images of CHIT/GOD@AgTNPs/ITO and CHIT/GOD/ITO have been presented (Supplementary data, Fig. 1S), which show no remarkable accumulation of AgTNPs and GOD.

3.2. Cyclic voltammetric characterization

Cyclic voltammetric (CV) experiment is used to evaluate the electrochemical performance of the electrodes. The CV experiments of different modified electrodes were performed in 5.0 mM potassium ferricyanide solution (supporting electrolyte: 0.1 M PB, pH 7.0). For the bare Pt electrode, the well-defined oxidation and reduction peaks caused by the $[Fe(CN)_6]^{3-}/[Fe(CN)_6]^{4-}$ redox couples are noticed in forward and reverse scan (curve *a*). After the electrode is modified by CHIT, an obvious decrease in reduction and oxidation peaks and a wide peak potential difference are observed (curve *b*). This may be due to the properties of the CHIT, as the organic membrane, which can block the electron transfer and increase the resistance between solution and the Pt electrode. When AgTNPs are embedded into the CHIT membrane, the current response of CVs could be increased and the peak potential difference could turn small (curve *c*), indicating the enhancing effect of the AgTNPs on the electric conductivity of the enzyme electrode. Meanwhile, a good performance of the fabricated CHIT/GOD@AgTNP/Pt electrode toward the oxidation of H_2O_2 makes it attractive for glucose sensing applications (Supplementary data, Fig. 2S).

3.3. Current response curves of the immobilized GOD electrode with AgTNPs

To evaluate the advantages of the AgTNPs modified biosensor, the comparison of the current response between GOD electrodes with 7×10^{-5} mg cm^{-2} and without AgTNPs was studied. As shown in Fig. 2, AgTNPs can dramatically enhance the current response of the electrode. For example, when glucose concentration is 1.0 mM, the current density of the electrode without nanorods is 4.07 μA cm^{-2}, and that of the electrode with gold nanorods is 67.17 μA cm^{-2}. These results prove that AgTNPs can play an important role in adsorption of enzyme due to their large specific surface area. Many reports (Chen et al., 1996; Katz et al., 2004) have given some evidence that the surface of nanomaterials would facilitate the immobilization of enzyme, and improve the activity and stability of the enzyme. In this system, AgTNPs could adsorb GOD molecules and then increase the response of the enzyme electrode. On the other hand, from cyclic voltammograms we know AgTNPs can improve the conductivity of the enzyme electrode. Therefore, the AgTNPs function as conducting leads between the enzyme and the electrode surface, and facilitate electron transfer between them, and then the capability of the biosensor can be improved. The effect of surface loading of AgTNPs also has been studied (Supplementary data, Fig. 3S), the current response of the

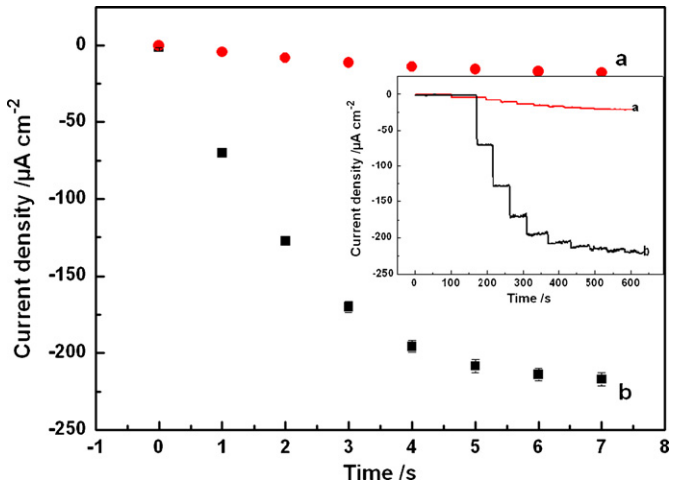

Fig. 2. Chronoamperometric current responses of electrodes: (a) CHIT/GOD/Pt and (b) CHIT/GOD@AgTNPs/Pt to successive addition of 1 mM glucose. Inset: plot of concentration of glucose (1–7 mM) vs. current; (a) CHIT/GOD/Pt and (b) CHIT/GOD@AgTNPs/Pt. The applied potential is 0.6 V vs. Ag/AgCl and the temperature is 35 °C.

biosensor in 1.0 mM glucose increases by the increasing of the loading of AgTNPs from 1×10^{-5} to 7×10^{-5} mg cm^{-2}. However, we find that when the loading of AgTNPs is more than 7×10^{-5} mg cm^{-2}, the response current tends to be saturated. Further increment of AgTNPs loading would be a waste of this expensive reagent, so in the following experiments the enzyme loading is set as 7×10^{-5} mg cm^{-2}.

3.4. Effect of applied potential and temperature on the glucose biosensor

To optimize the biosensor, the effect of applied potential and temperature on the biosensor response was studied (shown in Fig. 3A). The applied potential was evaluated at 1.0 mM glucose over the potential range from 0 to 0.8 V (incubation time: 1 min). When the applied potential increased from 0 to 0.6 V, the response current of the biosensor would accordingly increase. However, the current would decline when the applied potential exceeds 0.6 V. Therefore, a potential of 0.6 V is selected as the applied potential for amperometric measurement. Fig. 3B shows the effect of the temperature on GOD–AgTNPs biosensor. In 1.0 mM glucose solution, the temperature step increases from 0 to 70 °C. To our surprise, the current response of biosensor increases with temperature increasing from 0 to 60 °C, and then slightly declines. This result indicates that the enzyme bioconjugated with AgTNPs has good thermal stability (Supplementary data, Fig. 4S), which could benefit the preservation of enzyme electrode. To simulate the temperature of human body, temperature of 35 °C is selected for this work.

3.5. Biosensing performance

Under the optimized conditions, the performance of the prepared Pt/GOD@AgTNPs/CHIT electrode was examined. The amperometric responses and calibration curves are shown in Fig. 4, and the values of sensitivity, linear detection range (LDR), and limit of detection (LOD, $S/N = 3$) are listed in Table 1.

Fig. 4A shows the current response curves of GOD electrodes with AgTNPs in different concentrations of glucose. It can be seen that the electrode with AgTNPs can significantly enhance the current response.

The apparent Michaelis–Menten constant (K_M), which gives an indication of the enzyme–substrate, can be obtained from the Michaelis–Menten equation (Kong et al., 2009): $V = V_{max}[S]/(K_M + [S])$, where V is the rate of reaction, V_{max} is the maximum rate of reaction measured under saturated substrate condition, and $[S]$ is the bulk concentration of the substrate. The value of the apparent Michaelis–Menten constant (K_M) is calculated to show suitability of the enzyme in the hybrid nanobiocomposite matrix. From Fig. 4B, K_M value is found to be 2.35 mM for the immobilized GOD by using Lineweaver–Burk plot ($1/I$ versus $1/[C]$). The value of K_M is much lower than the reported ones 14.4 mM (Zou et al., 2008) and 6.3 mM (Qiu et al., 2008) by ferrocene-modified multiwalled carbon nanotube glucose biosensor and 3.73 mM by glucose biosensor based on Prussian blue/CHIT hybrid film (Wang et al., 2009). These results show that the biosensor possesses higher biological affinity to glucose.

3.6. Stability and interference of the enzyme electrode

The stability of the biosensor is investigated by amperometric measurements in the presence of 1 mM glucose. Fig. 5 shows that the current response of biosensor is retained about 80% of its original response after 50 times uninterrupted detection. In addition, the long-term stability is also tested by measuring the glucose concentration after a month. It is revealed that the current response of

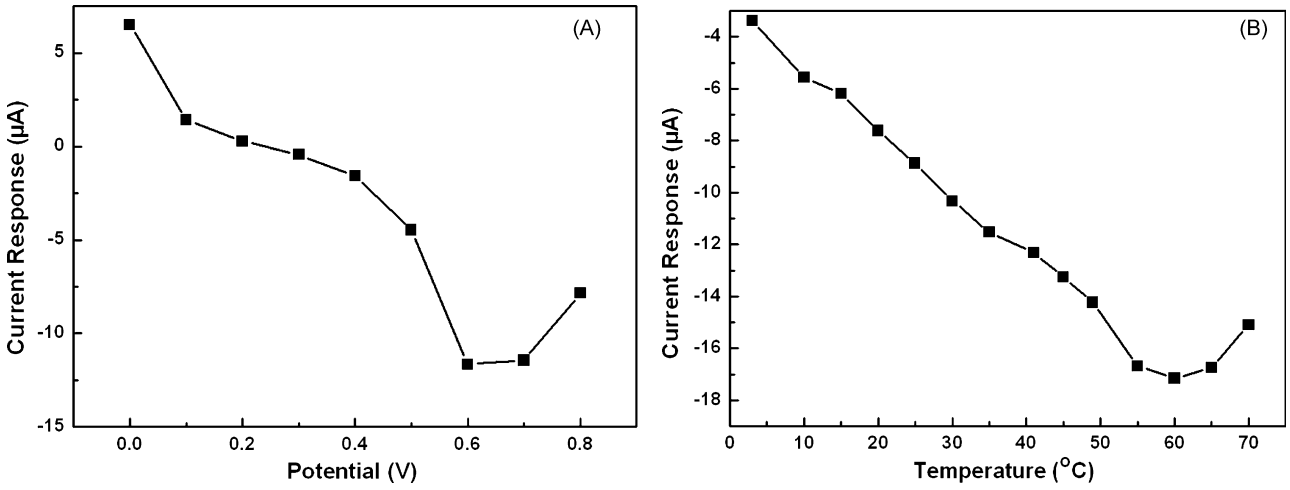

Fig. 3. Optimization of the biosensor: (A) the current response of the biosensor at 1 mM glucose with increasing potential. (B) The current response of the biosensor at 1 mM glucose with increasing temperature.

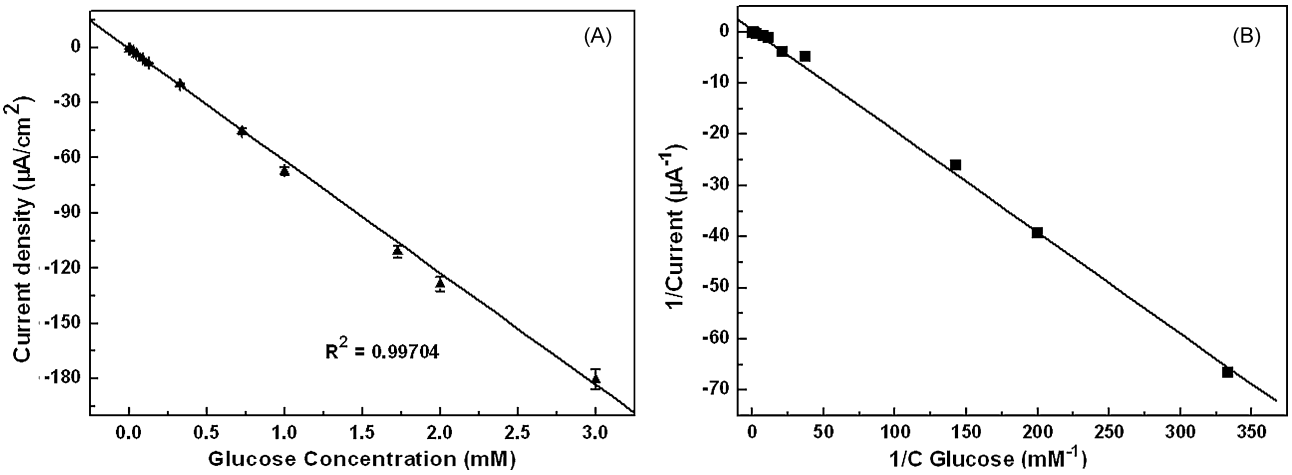

Fig. 4. (A) The calibration curve of the biosensor under the optimized conditions, (B) the kinetic analysis of electrocatalytic anodic currents at different glucose concentration according to Lineweaver–Burk equation.

Table 1
Construction and performance of several enzyme electrodes.

Protocol	Enzyme electrodes	Sensitivity/μA cm^{-2} mM^{-1}	LDR/μM	LOD/μM	References
Dipping/crosslinking	CHIT/GOD/Pt	4.07	50–3000	30	This work
Dipping/crosslinking	CHIT/GOD@AgTNPs/Pt	61.67	3–3000 (R^2 = 0.9991)	1	This work
Self-assembling	HFBI–GOD/Pt	4.21	500–20,000	90	Zhao et al. (2007)
Dip-coating	GOD/Pt/CNT/TiO_2	0.24	6–1500	5.7	Pang et al. (2009)
Layer-by-layer assembling	(PDDA/GOD)5/Nafion/PtC/GC	9.55	50–7000	20	Chen et al. (2007)
Drop-coating	(GOD)/graphene/CHIT	37.93	80–12,000	20	Kang et al. (2009)
Electrodeposition	CHIT–IL–GOD/nano–Au	14.3	3.0–9000	1.5	Zeng et al. (2009)
Crosslinking	CNT–Ptnano–GOD/GC	30	0.5–5000	0.5	Hrapovic et al. (2004)
Drop-coating	GOD/Au/CHIT–IL–MWNT(SH)		1000–10,000		Ragupathy et al. (2009)
Layer-by-layer assembling	$(CHIT/GOD)_n$/Au	15.9	2000–10,000		Miscoria et al. (2006)
Electrodeposition	GOD/CHIT/CNT/Au	6.7	5–8000	2	Zhou et al. (2007)
Layer-by-layer assembling	$(CHIT\text{-}g\text{-}PAN/GOD)_{12}$/Au		500–16,000		Xu et al. (2006)
Drop-coating	Graphene/AuNPs/CHIT/Au	17.5	2000–10,000	180	Shan et al. (2010)
Drop-coating	Nafion/GOD/graphene(Pt–Au)/GC	45.3	Up to 25,000	1	Baby et al. (2010)
Drop-coating	CHIT/$NiFe_2O_4$NPs/GOD/GCE	45.6	100–8000		Luo et al. (2010)

the sensor maintains 84% of the initial current response. This means that AgTNPs and CHIT films ensure well stability of the biosensor. With the help of AgTNPs and CHIT films, GOD can keep bioactivity on the Pt electrode.

The effect of some possible interfering compounds on the glucose biosensor was studied. 5 ppm of Fe^{3+}, Ni^{2+}, Cu^{2+}, Co^{2+}, Mn^{2+} and Zn^{2+} were negligible to determine 2.0 mM glucose. The interferences from ascorbic acid and uric acid were serious with even 20 μM of ascorbic acid and uric acid in 2 mM glucose.

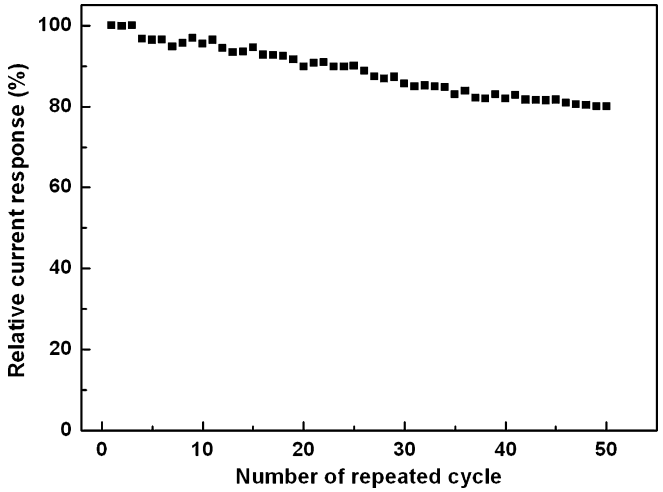

Fig. 5. The stability of the biosensor was investigated by amperometric measurements.

4. Conclusions

In summary, the addition of AgTNPs to an aqueous solution of CHIT and GOD has yielded new CHIT/GOD@AgTNPs/Pt glucose biosensor with GOD entrapped at high sensitivity. Due to their large surface-to-volume ratio and high conductivity, AgTNPs enhanced enzyme absorption and promoted electron transfer between redox enzymes and the surface of electrodes. The current response of modified electrode is much higher than that of without AgTNPs. The novel glucose biosensor showed relatively high sensitivity, broad linear range, low detection limit, good reproducibility, and long-term stability, high affinity to glucose of the GOD in the biocomposite. This composite film can easily extend to immobilize other biomolecules.

Acknowledgements

This study was supported by Funding Project for Academic human Resources Development in Institutions of Higher Learning Under the Jurisdiction of Beijing Municipality (PHR20100718) and Development Program of Science and Technology of Beijing Municipal Education Commission (KM200810028010).

Appendix A. Supplementary data

References

Ahmed, M.U., Hossain, M.M., Tamiya, E., 2008. Electroanalysis 20, 616–626.
Baby, T.T., Aravind, S.S.J., Arockiadoss, T., Rakhi, R.B., Ramaprabhu, S., 2010. Sens. Actuators B 145, 71–77.
Campbell, F.W., Belding, S.R., Baron, R., Xiao, L., Compton, R.G., 2009. J. Phys. Chem. C 113, 9053–9062.
Chen, X., Yan, X., Khor, K.A., Tay, B.K., 2007. Biosens. Bioelectron. 22, 3256–3260.
Chen, Z.J., Ou, X.M., Tang, F.Q., Jiang, L., 1996. Colloids Surf. B 7, 173–179.
Chi, Q.J., Zhang, J.D., Dong, S.J., Wang, E.K., 1994. J. Chem. Soc., Faraday Trans. 90, 2057–2060.
Courrol, L.C., Silva, F.R.O., Gomes, L., 2007. Colloids Surf. A 305, 54–57.
Dave, B.C., Dunn, B., Valentine, J.S., Zink, J.I., 1998. Oxford University Press, New York, pp. 113–134.
Drummond, T.G., Hill, M.G., Barton, J.K., 2003. Nat. Biotechnol. 21, 1192–1199.
Du, D., Chen, S.Z., Song, D.D., Li, H.B., Chen, X., 2008. Biosens. Bioelectron. 24, 475–479.
Gan, X., Liu, T., Zhong, J., Liu, X., Li, G., 2004. Chem. BioChem. 5, 1686–1691.
Grancharov, S.G., Zeng, H., Sun, S.H., Wang, S.X., O'Brien, S., Murray, C.B., Kirtley, J.R., Held, G.A., 2005. J. Phys. Chem. B 109, 13030–13035.
Haes, A.J., Van Duyne, R.P., 2002. J. Am. Chem. Soc. 124, 10596–10604.
Hrapovic, S., Liu, Y., Male, K.B., Luong, J.H.T., 2004. Anal. Chem. 76, 1083–1088.
Jiang, X.C., Yu, A.B., 2008. Langmuir 24, 4300–4309.
Kang, X.H., Wang, J., Wu, H., Aksayc, I.A., Liu, J., Lin, Y.H., 2009. Biosens. Bioelectron. 25, 901–905.
Katz, E., Willner, I., Wang, J., 2004. Electroanalysis 16, 19–44.
Kong, T., Chen, Y., Ye, Y.P., Zhang, K., Wang, Z.X., Wang, X.P., 2009. Sens. Actuators B 138, 344–350.
Krajewska, B., 2004. Enzyme Microb. Technol. 35, 126–139.
Lee, D., Lee, J., Kim, J., 2005. Adv. Mater. 17, 2828–2833.
Liang, H.P., Zhang, H.M., Hu, J.S., Guo, Y.G., Wan, L.J., Bai, C.L., 2004. Angew. Chem. Int. Ed. 43, 1540–1543.
Liu, Y., Wang, M.K., Zhao, F., Xu, Z.A., Dong, S.J., 2005. Biosens. Bioelectron. 21, 984–988.
Luo, L.Q., Li, Q.X., Xu, Y.H., Ding, Y.P., Wang, X., Deng, D.M., Xu, Y.J., 2010. Sens. Actuators B 145, 293–298.
Ma, S.Y., Lu, W.S., Mu, J., Liu, F., Jiang, L., 2008. Colloids Surf. A 324, 9–13.
Ma, S.Y., Mu, J., Qu, Y., Jiang, L., 2009a. Colloids Surf. A 345, 101–105.
Ma, Z.F., Si, G.L., Chu, Y.M., Chen, Y., 2009b. Prog. Chem. 21, 1847.
Miscoria, S.A., Desbrieres, J., Barrera, G.D., Labbé, P., Rivas, G.A., 2006. Anal. Chim. Acta 578, 137–144.
Pandey, P., Datta, M., Malhotra, B.D., 2008. Anal. Lett. 41, 159–209.
Pang, X., He, D., Luo, S., Cai, Q., 2009. Sens. Actuators B 137, 134–138.
Pastoriza-Santos, I., LizMarzán, L.M., 2002. Nano Lett. 2, 903–905.
Peng, S., Sun, S.H., 2007. Angew. Chem. Int. Ed. 46, 4155–4158.
Pingarron, J.M., Yanez-Sedeno, P., Gonzalez-Cortes, A., 2008. Electrochim. Acta 53, 5848–5866.
Qiu, J.D., Deng, M.Q., Liang, R.P., Xiong, M., 2008. Sens. Actuators B 135, 181–187.
Ragupathy, D., Gopalan, A.I., Lee, K.P., 2009. Electrochem. Commun. 11, 397–401.
Ren, X., Meng, X., Chen, D., Tang, F., Jiao, J., 2005. Biosens. Bioelectron. 21, 433–437.
Ren, X.L., Chen, D., Meng, X., Tang, F.Q., Du, A.M., Zhang, L., 2009. Colloids Surf. B 72, 188–192.
Shan, C.S., Yang, H.F., Han, D.X., Zhang, Q., Ivaskab, A., Niu, L., 2010. Biosens. Bioelectron. 25, 1070–1074.
Shimizu, M., Kobayashi, K., Morii, H., Mitsui, K., Knoll, W., Nagamune, T., 2003. Biochem. Biophys. Res. Commun. 310, 606–611.
Sorlier, P., Denuziere, A., Viton, C., Domard, A., 2001. Biomacromolecules 2, 765–772.
Thakar, R., Chen, Y.C., Snee, P.T., 2007. Nano Lett. 11, 3429–3432.
Wang, G., Xu, J.J., Ye, L.H., Zhu, J.J., Chen, H.Y., 2002. Bioelectrochemistry 57, 33–38.
Wang, X.Y., Gu, H.F., Yin, F., Tu, Y.F., 2009. Biosens. Bioelectron. 24, 1527–1530.
Wang, Z.L., Song, J.H., 2006. Science 312, 242–246.
Wen, D., Liu, Y., Yang, G.C., Dong, S.J., 2007. Electrochim. Acta 52, 5312.
Wen, X., Xie, Y.T., Mak, W.C., Cheung, K.Y., Li, X.Y., Renneberg, R., Yang, S., 2006. Langmuir 22, 4836–4842.
Willner, I., Willner, B., Katz, E., 2007. Bioelectrochemistry 70, 2–11.
Wu, T., Li, Y.F., Huang, C.Z., 2009. Chin. Chem. Lett. 20, 611–614.
Valentini, F., Palleschi, G., 2008. Anal. Lett. 41, 479–520.
Xiao, Y., Patolsky, F., Katz, E., Hainfeld, J.F., Willner, I., 2003. Science 299, 1877–1881.
Xue, C., Chen, X., Hurst, S.J., Mirkin, C.A., 2007. Adv. Mater. 19, 4071–4074.
Xu, X.H., Ren, G.L., Cheng, J., Liu, Q., Li, D.G., Chen, Q., 2006. J. Mater. Sci. 41, 4974–4977.
Yanez-Sedeno, P., Pingarron, J.M., 2005. Anal. Bioanal. Chem. 382, 884–886.
Zeng, X., Li, X., Xing, L., Liu, X., Luo, S., Wei, W., Kong, B., Li, Y., 2009. Biosens. Bioelectron. 24, 2898–2903.
Zhao, Z., Qiao, M., Yin, F., 2007. Biosens. Bioelectron. 22, 3021–3027.
Zhou, Q.M., Xie, Q.J., Fu, Y.C., Su, Z.H., Jia, X.E., Yao, Z., 2007. J. Phys. Chem. B 111, 11276–11284.
Zou, Y.J., Xiang, C.L., Sun, L.X., Xu, F., 2008. Biosens. Bioelectron. 23, 1010–1016.